

Article

Mono vs. Difunctional Coumarin as Photoinitiators in Photocomposite Synthesis and 3D Printing

Mahmoud Rahal^{1,2,3}, Haifaa Mokbel^{1,2}, Bernadette Graff^{1,2}, Joumana Toufaily³ ,
Tayssir Hamieh^{3,4} , Frédéric Dumur^{5,*}  and Jacques Lalevée^{1,2,*} 

¹ CNRS, IS2M UMR 7361, Université de Haute-Alsace, F-68100 Mulhouse, France; mahmoud-rahall@outlook.com (M.R.); haifaa.mokbel@uha.fr (H.M.); bernadette.graff@uha.fr (B.G.)

² Université de Strasbourg, 67081 Strasbourg, France

³ Laboratory of Materials, Catalysis, Environment and Analytical Methods (MCEMA) and LEADDER Laboratory, Faculty of Sciences, Doctoral School of Sciences and Technology (EDST), Lebanese University, Beirut 6573-14, Lebanon; joumana.toufaily@ul.edu.lb (J.T.); tayssir.hamieh@ul.edu.lb (T.H.)

⁴ SATIE-IFSTTAR, Université Gustave Eiffel, Campus de Marne-La-Vallée, F-78000 Versailles, France

⁵ CNRS, ICR UMR 7273, Aix Marseille Université, F-13397 Marseille, France

* Correspondence: frederic.dumur@univ-amu.fr (F.D.); jacques.lalevee@uha.fr (J.L.)

Received: 26 September 2020; Accepted: 13 October 2020; Published: 17 October 2020



Abstract: This work is devoted to investigate three coumarin derivatives (Coum1, Coum2, and Coum3), proposed as new photoinitiators of polymerization when combined with an additive, i.e., an iodonium salt, and used for the free radical polymerization (FRP) of acrylate monomers under mild irradiation conditions. The different coumarin derivatives can also be employed in three component photoinitiating systems with a Iod/amine (ethyl 4-dimethylaminobenzoate (EDB) or N-phenylglycine (NPG)) couple for FRP upon irradiation with an LED @ 405 nm. These compounds showed excellent photoinitiating abilities, and high polymerization rates and final conversions (FC) were obtained. The originality of this work relies on the comparison of the photoinitiating abilities of monofunctional (Coum1 and Coum2) vs. difunctional (Coum3) compounds. Coum3 is a combined structure of Coum1 and Coum2, leading to a sterically hindered chemical structure with a relatively high molecular weight. As a general rule, a high molecular weight should reduce the migration of initiating molecules and favor photochemical properties such as photobleaching of the final polymer. As attempted, from the efficiency point of view, Coum3 can initiate the FRP, but a low reactivity was observed compared to the monofunctional compound (Coum1 and Coum2). Indeed, to study the photochemical and photophysical properties of these compounds, different parameters were taken into account, e.g., the light absorption and emission properties, steady state photolysis, and fluorescence quenching. To examine these different points, several techniques were used including UV-visible spectroscopy, real-time Fourier Transform Infrared Spectroscopy (RT-FTIR), fluorescence spectroscopy, and cyclic voltammetry. The photochemical mechanism involved in the polymerization process is also detailed. The best coumarins investigated in this work were used for laser writing (3D printing) experiments and also for photocomposite synthesis containing glass fibers.

Keywords: free radical polymerization; mild irradiation conditions; coumarins; composite materials; LED; 3D printing

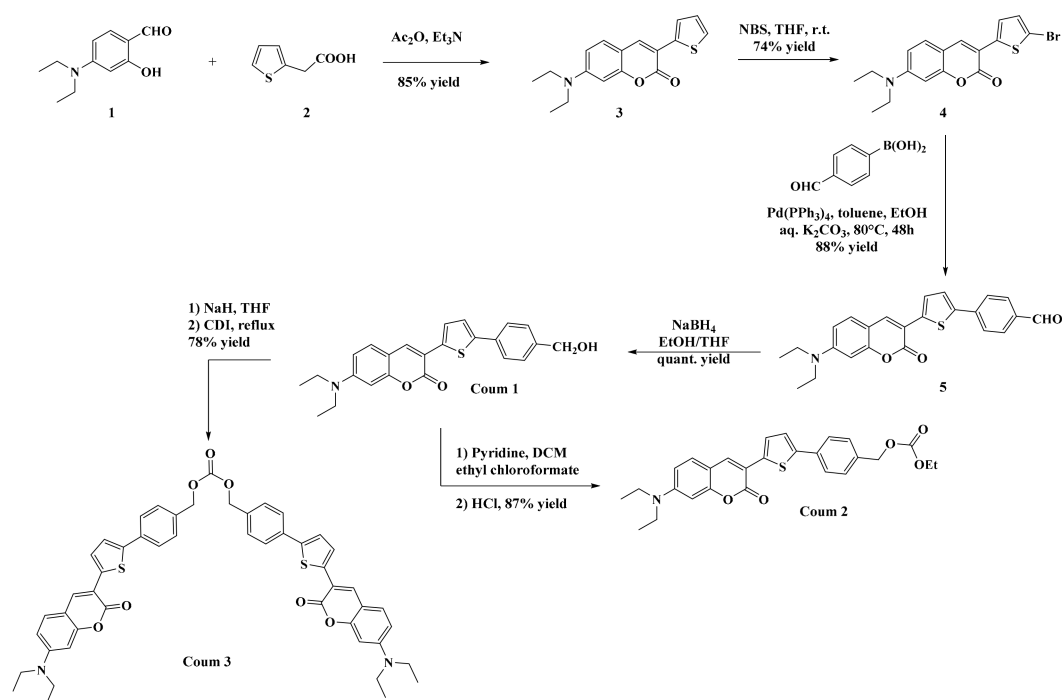
1. Introduction

During the last decade, photochemical reactions showed a huge number of industrial and academic applications such as UV-curing, solar cells, and photopolymerization [1,2]. These reactions can advantageously replace thermally-based chemical processes due to their many advantages [3,4] such

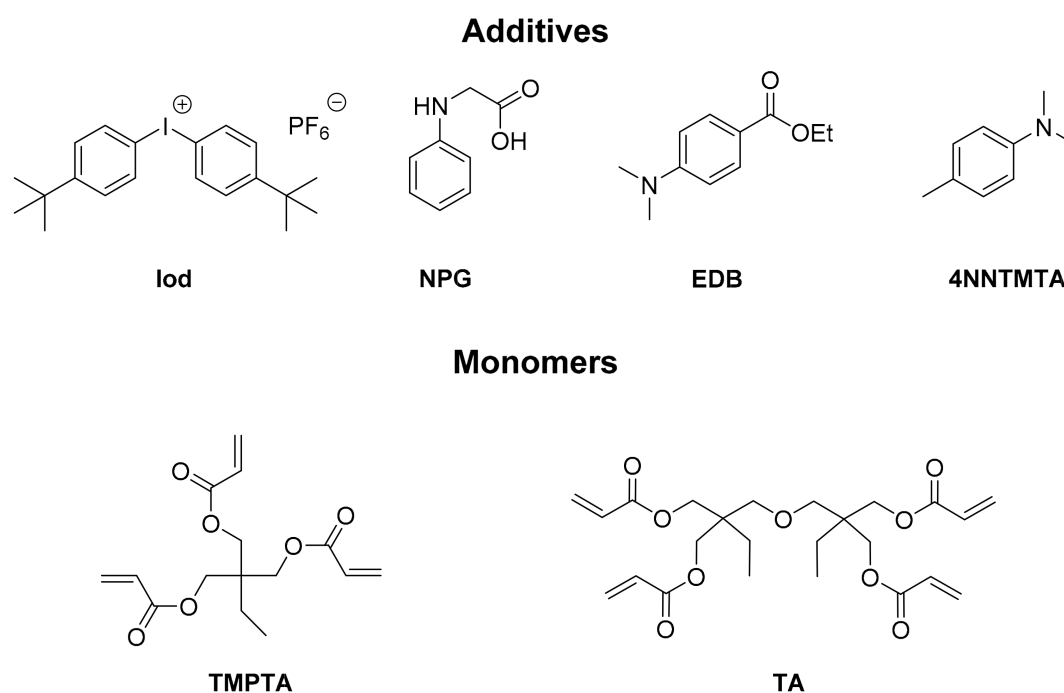
as low-cost reactions, low energy consumption, and very fast reaction (a few seconds) processes while exhibiting an eco-friendly character [5]. Therefore, the development of photosensitive systems with low toxicity will be preferably retained for the design of new initiating systems under mild irradiation conditions. Coumarin and its derivatives form a class of natural compounds that exhibit biological activity, e.g., cytotoxic activity against several human tumor cell lines [6,7], as well as spasmolytic, antiarrhythmic [8], and antioxidant [9] activities. Coumarins are also used in flavoring food and in cosmetic products such as fragrances [10,11]. These compounds are also characterized by high photoluminescence quantum yields and can therefore be used as fluorescent chromophores for various applications [12]. Recently, heterocyclic fluorescent compounds have been used in several research fields such as molecular probes for biochemical research [13], emitters for electroluminescent devices [14], fluorescent probes for heavy metal sensing [15], molecules exhibiting biological activities [16] or active layers for photovoltaic applications [17].

In fact, recent research devoted to photopolymerization aims at developing chromophores capable of strong absorption in the visible range [18–22]. For more safety and less harmfulness while reducing the energy consumption, light-emitting diodes (LEDs) [23] are now classically used in photopolymerization, enabling a good overlap between the emission of the LEDs and the absorption spectra of the photoinitiators (PIs).

In this work, three coumarins (Coum1, Coum2, and Coum3) bearing different substituents were synthesized and characterized (See Scheme 1). These coumarins were notably used in two (Coum/Iod (0.1%/1% *w/w*)) and three (Coum/Iod/amine (0.1%/1%/1% *w/w/w*)-component photoinitiating systems (PIS) to generate reactive species with the different additives presented in Scheme 2. Excellent polymerization initiating abilities were found at 405 nm during the free radical polymerization (FRP) of acrylates. In fact, the different substituents of coumarins could drastically affect the photochemical and/or electrochemical properties and absorption properties and thus their abilities to initiate the photopolymerization process. These coumarins were used in 3D printing application upon irradiation at 405 nm. The formation of composite materials using glass fibers was also provided. These different applications clearly highlight the remarkable performances of the different coumarins reported in this work as photoinitiators.



Scheme 1. The different coumarins (Coum1, Coum2, and Coum3) investigated in this study.



Scheme 2. Other chemical compounds used in this work.

Indeed, the reaction mechanisms can be explained using several techniques such as cyclic voltammetry, absorption, and photoluminescence techniques, or real-time Fourier transform infrared spectroscopy (RT-FTIR).

2. Results

2.1. Free Radical Photopolymerization (FRP) of Acrylate Monomers (TMPTA or Di(trimethylolpropane) Tetraacrylate (TA))

Thanks to their excellent absorption properties, these coumarins showed a very high performance (Figure 1, Table 1) in terms of final conversions and rates of polymerization upon exposure to the LED @ 405 nm. In fact, Iod alone, NPG alone, or Coum alone did not work. Conversely, two- or three-component systems such as Coum/Iod (0.1%/1% *w/w*) or Coum/Iod/amine (0.1%/1%/1% *w/w/w*) were quite efficient and could efficiently initiate the polymerization process. Obviously, this is related to the photooxidation process between Iod and coumarin (electron transfer from Coum* to Iod) and to the formation of a charge transfer complex (CTC) between Iod and NPG [Iod-NPG]_{CTC}.

Table 1. Final conversions of the acrylate function for TA using different PIS (400 s of irradiation, LED @ 405 nm, sample thickness = 1.4 mm).

| Two-Component Photoinitiating System Coum/Iod (0.05%/1% <i>w/w</i>) and Coum/Iod (0.1%/1% <i>w/w</i>) | | | Three-Component Photoinitiating System Coum/Iod/EDB and Coum/Iod/NPG (0.1%/1%/1% <i>w/w/w</i>) | | |
|---|------------------|-------------------|---|------------------|------------------|
| Coum1/Iod | Coum2/Iod | Coum3/Iod | Coum1/Iod/amine | Coum2/Iod/amine | Coum3/Iod/amine |
| 83% ¹ | 71% ¹ | n.p. ¹ | 84% ³ | 83% ³ | 59% ³ |
| 73% ² | 83% ² | 32% ² | 90% ⁴ | 89% ⁴ | 78% ⁴ |

¹ Coum/Iod (0.05%/1% *w/w*); ² Coum/Iod (0.1%/1% *w/w*); ³ Coum/Iod/EDB (0.1%/1%/1% *w/w/w*); ⁴ Coum/Iod/NPG (0.1%/1%/1% *w/w/w*); n.p.: no polymerization.

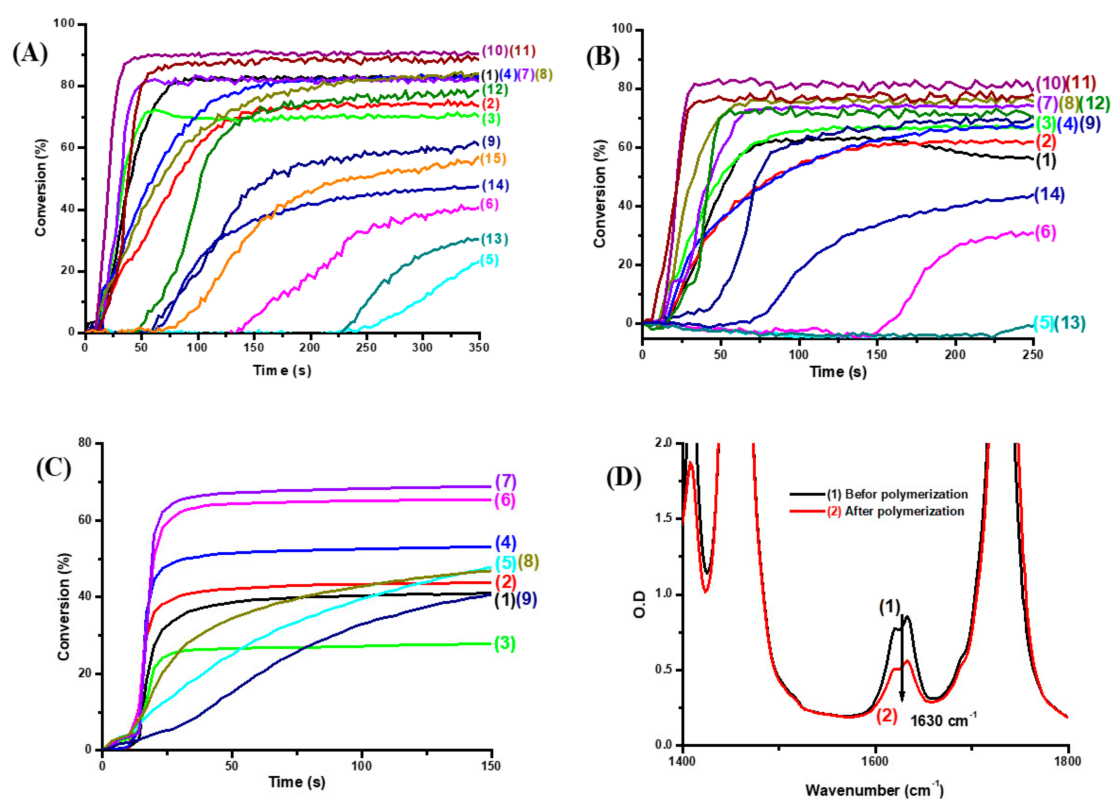


Figure 1. Polymerization profiles (acrylate function conversion vs. irradiation time) for TA (A) and TMPTA (B) (thickness = 1.4 mm in laminate) upon exposure to the LED @ 405 nm in the presence of the two- and three-component photoinitiating systems: (1) Coum 1/Iod (0.05%/1% *w/w*), (2) Coum 1/Iod (0.1%/1% *w/w*), (3) Coum 2/Iod (0.05%/1% *w/w*), (4) Coum 2/Iod (0.1%/1% *w/w*), (5) Coum 3/Iod (0.05%/1% *w/w*), (6) Coum 3/Iod (0.1%/1% *w/w*), (7) Coum 1/Iod/EDB (0.05%/1%/1% *w/w/w*), (8) Coum 2/Iod/EDB (0.05%/1%/1% *w/w/w*), (9) Coum 3/Iod/EDB (0.05%/1%/1% *w/w/w*), (10) Coum 1/Iod/NPG (0.05%/1%/1% *w/w/w*), (11) Coum 2/Iod/NPG (0.05%/1%/1% *w/w/w*), (12) Coum 3/Iod/NPG (0.05%/1%/1% *w/w/w*), (13) Iod/EDB (1%/1% *w/w*), (14) Iod/NPG (1%/1% *w/w*) and (15) Coum 3/Iod (0.05%/1% *w/w*) with 5 drops of chloroform. (C) Polymerization profiles (acrylate function conversion vs. irradiation time) for TMPTA (thickness = 25 μm in laminate) upon exposure to the LED @ 405 nm in the presence of two- and three-component photoinitiating systems: (1) Coum 1/Iod (0.05%/1% *w/w*), (2) Coum 1/Iod (0.1%/1% *w/w*), (3) Coum 2/Iod (0.05%/1% *w/w*), (4) Coum 2/Iod (0.1%/1% *w/w*), (5) Coum 3/Iod (0.1%/1% *w/w*), (6) Coum 1/Iod/NPG (0.1%/1%/1% *w/w/w*), (7) Coum 2/Iod/NPG (0.1%/1%/1% *w/w/w*), (8) Coum 3/Iod/NPG (0.1%/1%/1% *w/w/w*) and (9) Iod/NPG (1%/1% *w/w*). (D): IR spectra obtained before and after polymerization for Coum 1/Iod/NPG (0.05%/1%/1% *w/w/w*) in TMPTA (thickness = 25 μm).

For the photopolymerization of di(trimethylolpropane) tetraacrylate (TA) in thick samples in laminate (1.4 mm thickness), an excellent polymerization efficiency was found using Coum/Iod or Coum/Iod/NPG when irradiated with an LED @ 405 nm (See Figure 1A). High final conversions were obtained: the FC could increase up to 90 % for coum2/Iod/NPG (0.1%/1%/1% *w/w/w*) compared to 83% using coum2/Iod (0.1%/1% *w/w*). These results show the superiority of the three-component systems over their two-component PIS analogues (See Figure 1C). Indeed, in the case of the three-component systems, the additional amines (NPG, EDB) are introduced in order to regenerate the photosensitizer, enabling a photocatalytic system. For the two-component systems, the photosensitizer is irreversibly oxidized upon photoexcitation, resulting from an electron transfer in the excited state from the photosensitizer to the photoinitiator (Iod) so that an irreversible consumption of the photosensitizer is observed [24,25]. This issue is addressed by the introduction of a sacrificial amine in the three-component systems. The same behavior is also observed with coum1 (Figure 1, curve 1 for the two-component PIS coum1/Iod (0.05%/1% *w/w*) and curve 10 for the three-component PIS coum1/Iod/NPG (0.05%/1%/1%

$w/w/w$). Besides, it has to be noticed that a smaller enhancement of the final monomer conversion is observed with this second coumarin. Thus, if a monomer conversion of 84% is observed for the three-component system coum1/Iod/NPG (0.05%/1%/1% $w/w/w$), the monomer conversion is in turn comparable to that obtained with the two-component system (83% monomer conversion (See Table 1). The crucial role of coumarins in the final monomer conversions is clearly evidenced through the different photopolymerization experiments.

In fact, in the case of Coum2 and 3, the increase in the concentration induces an increase in the final conversion rate (Figure 1A. Curve 3 and 4 for Coum2, and Curve 5 and 6 for Coum3); this can be explained by a greater generation of radicals. Conversely, a lower conversion rate is observed by increasing the concentration in the case of Coum1 (See Figure 1A Curve 1 and 2); this is due to an inner filter effect which prevents the penetration of light to the depth.

The performance of the different photoinitiating systems for the FRP of acrylates in thin films and under laminated conditions was also relatively good (See Figure 1B). In this case, the addition of NPG clearly showed an influence on the polymerization profile: the FC could increase up to 69.4% for Coum2/Iod/NPG compared to 53.4% with the two-component Coum2/Iod (0.1%/1% w/w) system. Similarly, the FC increased up to 63% with the three-component coum1/Iod/NPG (0.05%/1%/1% $w/w/w$) system, far from the result obtained with the two-component coum1/Iod (0.05%/1% w/w) system (41.3%).

The trend detected for the FRP of the acrylic monomers (TMPTA and TA) for thick samples and under laminated conditions followed relatively the same order: Coum1 and Coum 2 are the best candidates for the FRP in three-component PIS; Coum/Iod/NPG. Interestingly, the reactivity of PIS comprising NPG as the amine was higher than that comprising EDB (e.g., Figure 1A. Curve 10 vs. Curve 7). Besides, the polymerization was still possible with this second amine. The difference in reactivity between NPG and EDB can be attributed to the fast decarboxylation of NPG when used as the sacrificial amine. This decreases the possibility of back electron transfer while jointly increasing the reactivity. Tack-free coatings were obtained in most of the cases, in full agreement with the increase in the characteristic acrylate peak at 1630 cm^{-1} for thin samples recorded before and after irradiation (See Figure 1D).

2.2. 3D-Printing Experiments Using Coum/Iod or Coum/Iod/4-N,N,TMA Systems

Some examples of 3D patterns obtained by irradiation with a laser diode emitting at 405 nm (spot size: 50 μm) are presented in Figure 2. The three-component photoinitiating systems based on Coum1 and Coum2 (Coum1–2/Iod or coum1–2/Iod/amine) were very reactive to initiate the FRP of TMPTA and TA under air conditions. Remarkably, the high reactivity of the different resins allowed efficient polymerization in the irradiated zones; 3D patterns elaborated with remarkable precision were obtained using laser writing. In particular, these patterns were prepared in a relatively short space of time (~2 min) while enabling a high spatial resolution. 3D polymer patterns were characterized using a numerical optical microscope, as shown in Figure 2.

2.3. LED Conveyor Experiments for Composite Preparation

Photocomposite materials were produced by irradiation using an LED @ 385 nm (0.7 W/cm^2) using three-component PIS based on Coum2/Iod/NPG (0.1%/1%/1% $w/w/w$) or Coum1/Iod/NPG (0.1%/1%/1% $w/w/w$). Composite materials were prepared by impregnation of glass fibers (one layer, thickness = 2 mm) with an acrylic organic resin (50% organic resin/ 50% glass fibers). Interestingly, fast polymerization was observed using different PIS, where the surface and also the bottom became tack-free after only one pass using one layer of glass fibers. The results reported in Figure 3 show that coumarin derivatives have a high reactivity to produce photocomposite materials at 385 nm. In particular, an excellent depth of cure could be determined for all samples.

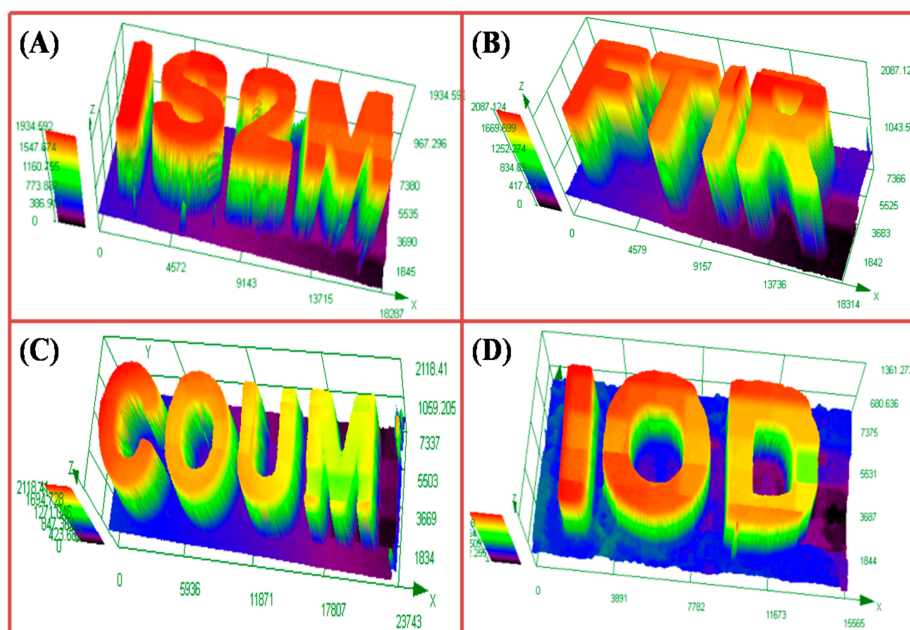


Figure 2. Characterization of the 3D patterns by numerical optical microscopy; (A) Coum2/Iod/4-N,N TMA (0.024%/0.4%/0.16% $w/w/w$) in TA; (B) Coum1/Iod/4-N,N TMA (0.02%/0.4%/0.16% $w/w/w$) in TA; (C) Coum2/Iod (0.02%/0.4% w/w) in TMPTA, (D) Coum1/Iod (0.02%/0.4% w/w) in TMPTA.

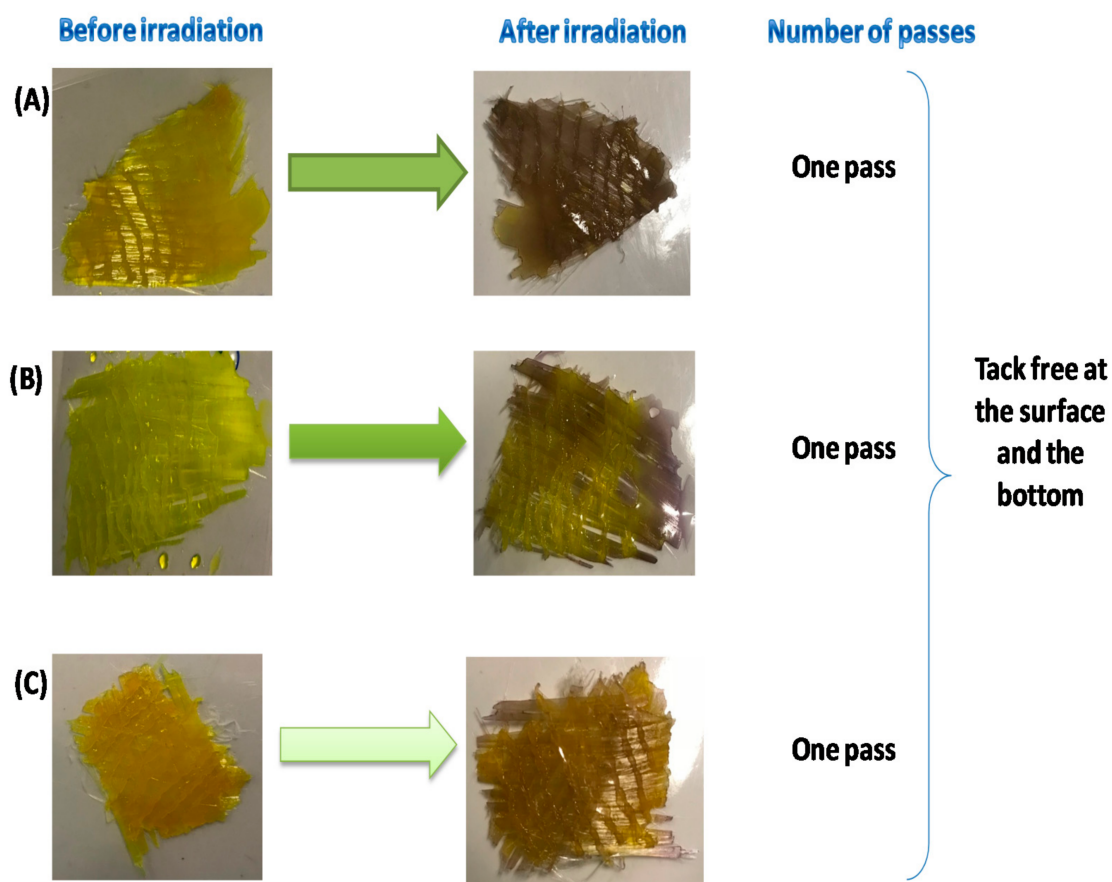


Figure 3. Photocomposite synthesis, Belt Speed = 2 m/min, using LED @ 385 nm: (A) Coum1/Iod/NPG (0.1%/1%/1% $w/w/w$) in TA, (B) Coum2/Iod/NPG (0.1%/1%/1% $w/w/w$) in TMPTA and (C) Coum1/Iod/NPG (0.1%/1%/1% $w/w/w$) in TMPTA.

3. Discussion

Based on the photochemical reactivity as well as the practical efficiency of the investigated coumarins that was clearly demonstrated, their associated chemical mechanisms have been investigated in detail.

3.1. Light Absorption Properties of the Different Dyes

Absorption spectra of coumarin derivatives investigated in this work are shown in Figure 4 (See Table 2). The different absorption spectra are characterized by two main absorption bands, one located in the near-UV range (<350 nm) and a second one with the highest molar extinction coefficient detected in the 350–550 nm range (e.g., Coum1 $\sim 23,000 \text{ M}^{-1} \text{ cm}^{-1}$ @ 405 nm and $\sim 43,560 \text{ M}^{-1} \text{ cm}^{-1}$ @ λ_{max} i.e., (444 nm)). Molar extinction coefficients of coumarins followed this order at the absorption maxima: $\epsilon_{\text{Coum2}} > \epsilon_{\text{Coum3}} > \epsilon_{\text{Coum1}}$. The difference between the extinction coefficients of these compounds is related to the substitution of the coumarin scaffold. Remarkably, their absorption range extends between 350 and 520 nm. Therefore, a good overlap of their absorption spectra with the emission spectrum of the LED @ 405 nm used in this work could be achieved. Optimized geometries as well as the contour plots of the highest occupied molecular orbital (HOMO) and the lowest unoccupied molecular orbital (LUMO) are presented in Figure 5. As shown in Figure 5, HOMO and LUMO energy levels extend over the entire π -conjugated system. More precisely, the HOMO energy level comprises the coumarin moiety as well as the electron-rich thiophene.

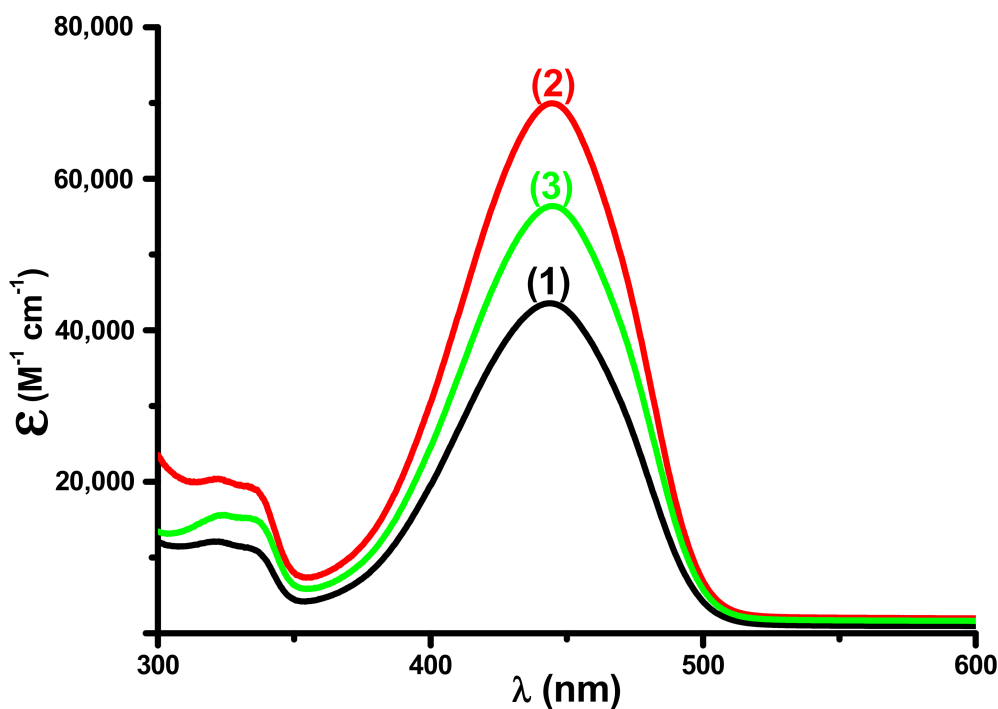


Figure 4. UV-visible absorption spectra in chloroform: (1) Coum1, (2) Coum2 and (3) Coum3.

Table 2. Light absorption properties of coumarin compounds at 405 nm and $\lambda_{\mu\alpha\zeta}$.

| - | λ_{max} (nm) | ϵ_{max} ($\text{M}^{-1} \text{ cm}^{-1}$) | $\epsilon_{@ 405 \text{ nm}}$ ($\text{M}^{-1} \text{ cm}^{-1}$) |
|-------|-----------------------------|---|---|
| Coum1 | 444 | 43,500 | 23,000 |
| Coum2 | 444 | 69,900 | 35,900 |
| Coum3 | 445 | 56,400 | 28,900 |

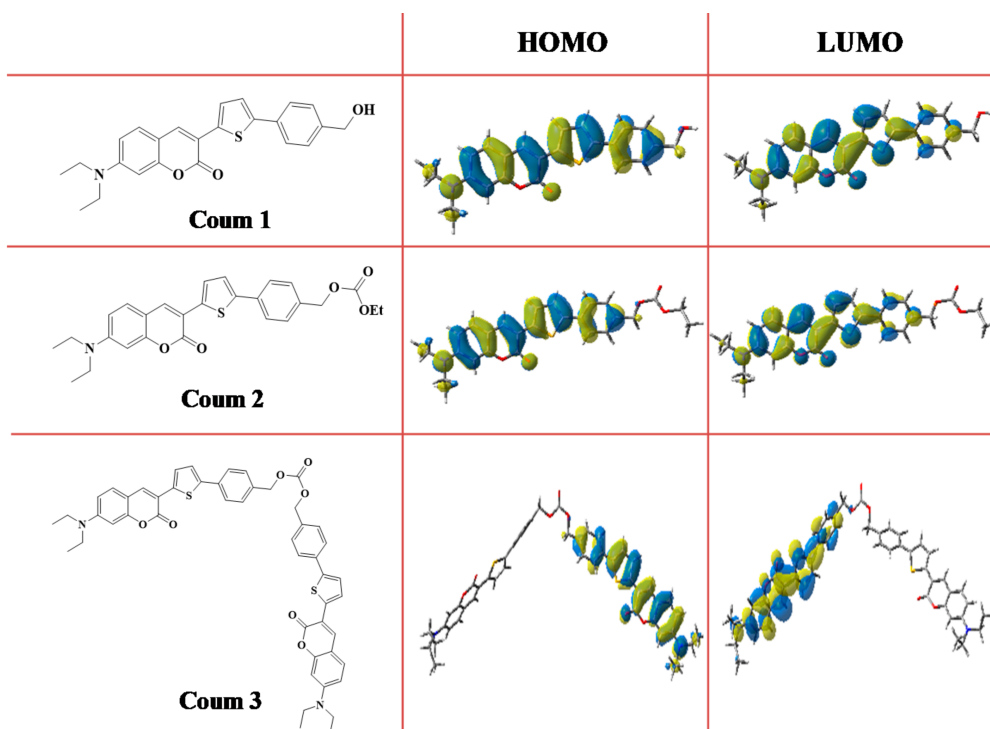


Figure 5. HOMO and LUMO energy levels of Coum1–Coum3 at the UB3 LYP/6–31G* level.

3.2. (Photo)Chemical Mechanisms

The chemical mechanisms were investigated more in detail for Coum3 used as a reference structure and compared to those of Coum1 and Coum2.

3.2.1. Photophysical and Photochemical Properties of Coum3

Steady-state photolysis experiments of Coum3 were carried out using UV-visible spectroscopy. The steady state photolysis of Coum3/Iod (10^{-2} M) in chloroform was very fast compared to the high photostability of Coum3 alone (e.g., Coum3/Iod in Figure 6D(2) vs. Coum3 alone in Figure 6D(1) upon irradiation with the LED @ 375 nm. Indeed, the consumption of Coum3 with Iod (10^{-2} M) (Figure 6D(3) Consumption = 91%) was greater than that of Coum3/Iod/EDB (86%); these results are explained by a weaker regeneration of coum3 in the presence of the three-component PI. Fluorescence experiments of Coum3 in chloroform are shown in Figure 6A. The crossing point of the absorption and fluorescence spectra enables us to determine the first singlet excited state energies (E_{S1}) (e.g., estimation of E_{S1} for Coum3: 2.53 eV; Table 3, Figure 6C). As an indicator of interaction occurrence, fast fluorescence quenching processes of Coum3 by Iod were also detected (See Figure 6A and Table 3); this clearly shows a very important interaction of Coum3 (and even for Coum1 and 2) with Iod. These results show a very high quantum yield (for example, $\phi = 0.76$ for Coum3, Table 3).

Table 3. Parameters characterizing the chemical mechanisms associated with the $^1\text{Coum/Iod}$ interaction in acetonitrile.

| - | E_{ox} (eV) | E_{S1} (eV) | ΔG_{S1} (eV) | K_{SV} | $\Phi_{et(\text{Coum/Iod})}$ |
|-------|---------------|---------------|----------------------|----------|------------------------------|
| Coum1 | 0.87 | 2.54 | −1.46 | 20 | 0.37 |
| Coum2 | 0.86 | 2.56 | −1.49 | 93 | 0.87 |
| Coum3 | n.o | 2.53 | - | 121 | 0.76 |

E_{S1} : singlet excited state energy, ΔG_{S1} : Free energy change of the singlet state $\Phi_{et(\text{Coum/Iod})}$: electron transfer quantum yields.

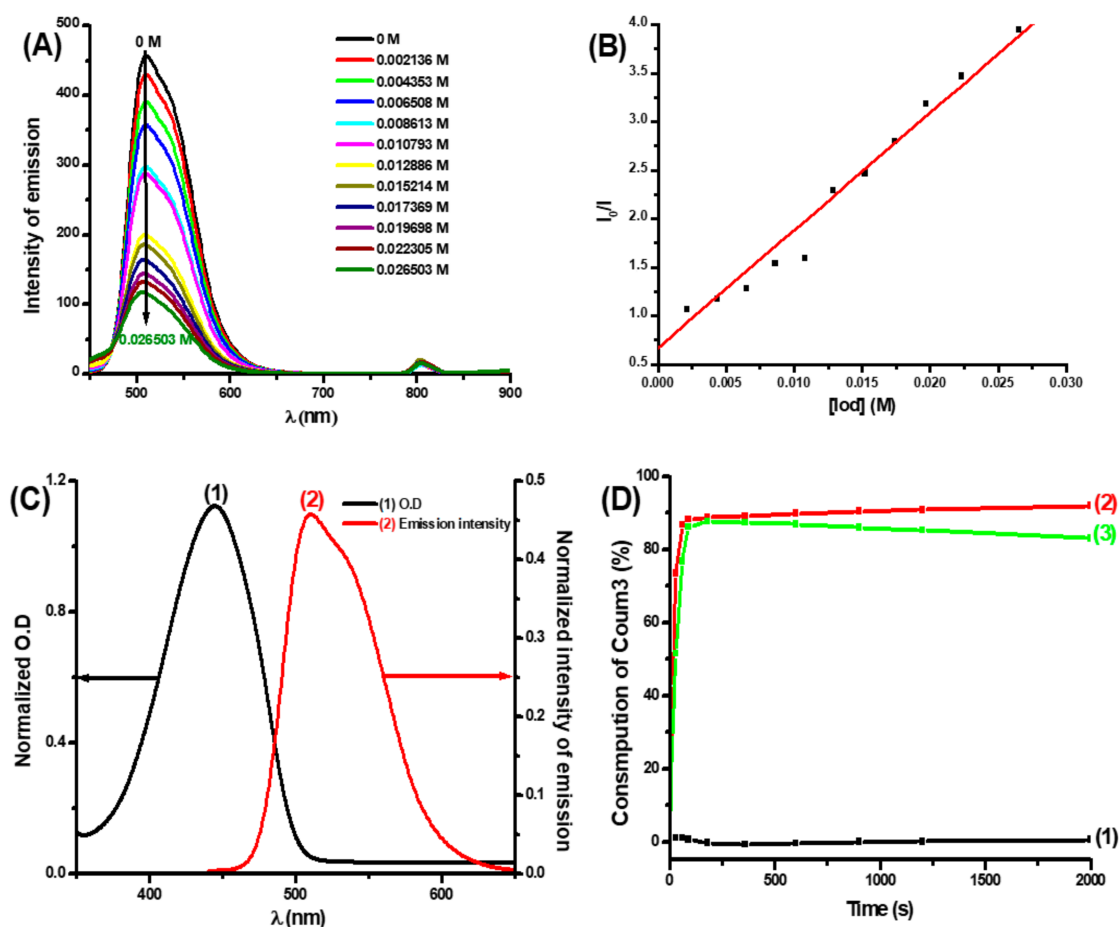


Figure 6. (A) Quenching of Coum3 by Iod, (B) Determination of the Stern–Volmer coefficient, (C) Determination of ES1, (D) Consumption of Coum3: (1) Without Iod, (2) With Iod (10^{-2} M), and (3) With Iod/EDB vs. irradiation time upon exposure to the LED @ 375 nm in chloroform.

3.2.2. Photophysical Properties of Coumarins Coum1 and Coum2

Steady-state photolysis experiments of coumarin derivatives (e.g., Coum2) alone, with Iod or Iod/EDB are reported in Figure 7. Interestingly, photolysis of the Coum2/Iod (See Figure 7B) system was faster than that determined for Coum2 alone (See Figure 7A), which proved to be highly photostable. The Coum2/Iod interaction showed a photo-oxidation process (electron transfer from coum2 to Iod). In particular, the formation of a photoproduct exhibiting an absorption in the 500–650 nm range could be formed by the interaction of Coum2 with Iod (See Figure 7B). These results clearly show the effect of iodonium on the photolysis of coum2 and therefore on the generation of radicals, because once the Coum2 is irradiated, it reaches an excited state, where an electron transfer from Coum2 to iodonium salt can occur.

On the other hand, photolysis of Coum2 with Iod/EDB (See Figure 7C) was also very fast, but the percentage of consumption (vs. time of irradiation) was lower than that of Coum2/Iod; this result can be attributed to the regeneration of PI in the presence of the three-component PIS (See Figure 7D).

The percentage of consumption was very high for the different coumarins in the presence of Iod (85% for Coum1, 91% for Coum2, and 93% for Coum3), but this percentage decreased remarkably in the presence of Iod/EDB (70% for Coum1, 72% for Coum2, and 83% for Coum3); this decrease was due to the partial regeneration of these coumarins in the three-component systems.

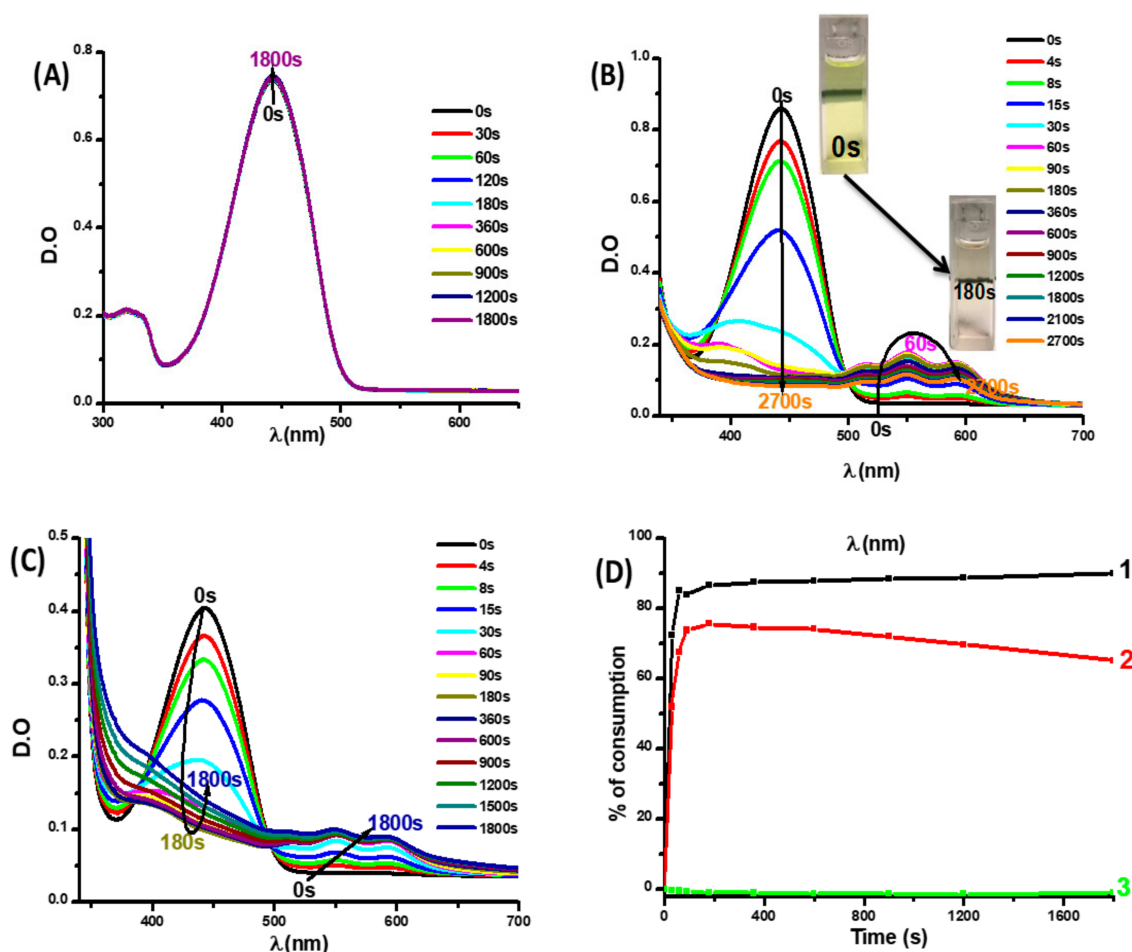


Figure 7. Photolysis of Coum2 in acetonitrile upon exposure to the LED @ 405 nm: (A) Coum2 alone (B): With Iod (10^{-2} M); and (C) With Iod/EDB (10^{-2} M). (D) Consumption of Coum2: (1) With Iod, (2) With Iod/EDB, and (3) Without Iod vs. irradiation time upon exposure to the LED @ 375 nm in chloroform.

3.2.3. Fluorescence Quenching Experiments and Cyclic Voltammetry Measurements

Emission and fluorescence quenching spectra of coumarins in chloroform (e.g., Coum2) are presented in Figure 8. The crossing point of the emission and absorption spectra allows the determination of E_{S1} (singlet excited state energy), e.g., $E_{S1} = 2.54$ eV for Coum1, and 2.56 eV for Coum2. In fact, the fluorescence quenching of Coum2/Iod was very fast and was characterized by high Stern–Volmer coefficients. Thus, very high electron transfer quantum yields ($\phi_{et} = 0.37$ for Coum1 and 0.87 for Coum2) were determined. While no quenching was observed in the presence of EDB, there was an increase of the emission intensity that can be ascribed to the formation of a complex between Coum and EDB. This result is totally in agreement with that of the photopolymerization process of Coum/EDB (or NPG). The electron transfer quantum yields (ϕ_{et}) were determined according to the following equation:

$$\phi_{S1} = K_{SV}[Iod]/(1 + K_{SV}[Iod]) \quad (1)$$

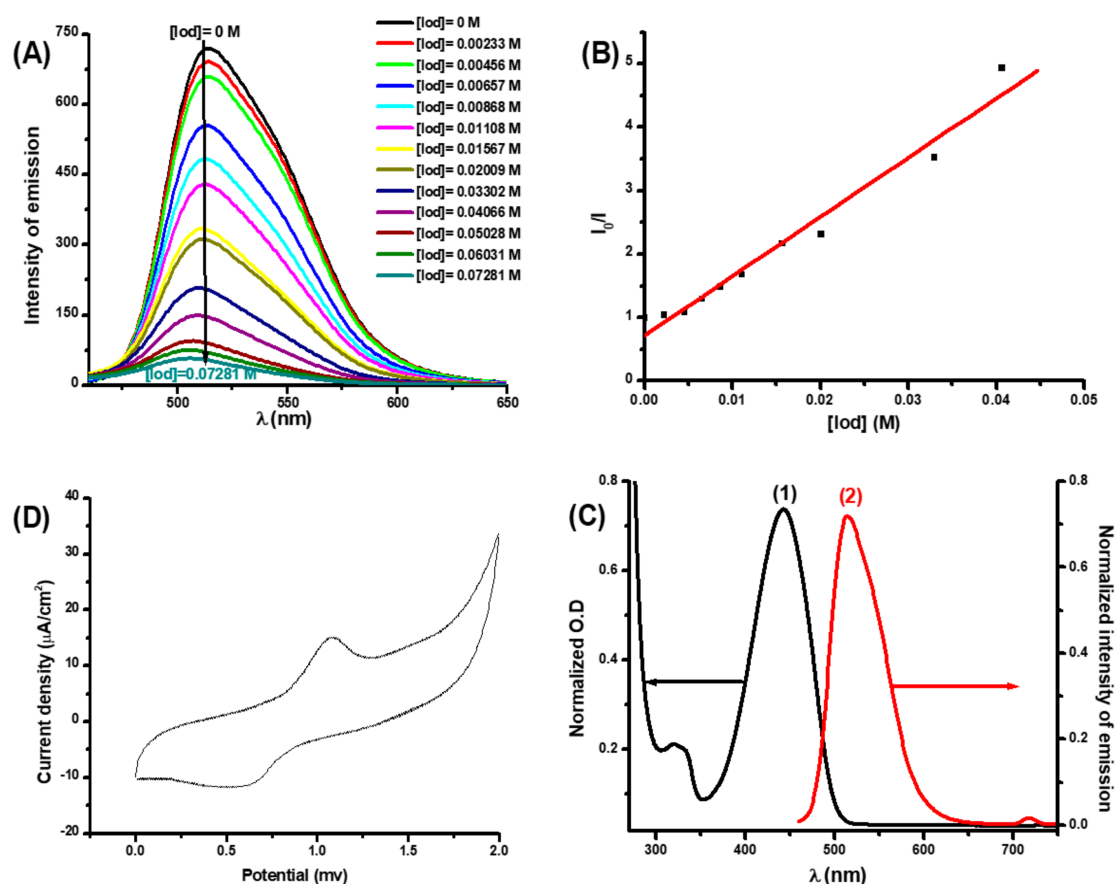
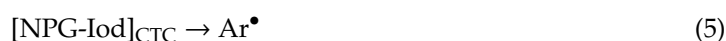
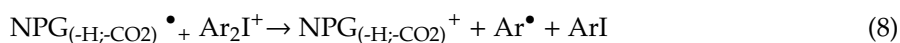
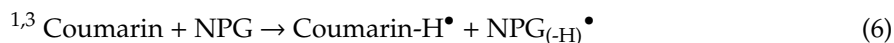


Figure 8. (A) Fluorescence quenching of Coum2 by Iod, (B) Determination of the Stern–Volmer coefficient, (C) ES1 determination, and (D) Cyclic voltammetry of Coum2 in acetonitrile.

This term characterizes the formation of reactive species (Ar^\bullet and $\text{PI}^{\bullet+}$) capable of initiating the FRP process. Electrochemical properties of the different coumarins were also examined by cyclic voltammetry (Figure 8D), and highly favorable free energy changes ΔG_{et} (which were calculated from Rhem–Weller equation using the oxidation potential between coumarin and Iod, and E_{S1}) could be determined, e.g., $\Delta G_{\text{et}} = -1.46$ eV for Coum1 and -1.5 eV for Coum2.

Photopolymerization results can be explained by a global chemical mechanism, based on the results obtained through the different experiments above including fluorescence quenching, electrochemical, and photolysis experiments. Firstly, once the coumarins absorb the incident light, coumarins are promoted in an excited state PI^* , and reactive species (Ar^\bullet and $\text{Coum}^{\bullet+}$) are generated by the interaction between Coum^* and Iod salt (r2). A charge transfer complex (CTC) can also be obtained due to the Iod/NPG interaction, so that Ar^\bullet are formed (r3–r4). In addition, a hydrogen atom transfer from NPG to PI can also occur so that two different types of radicals can be generated (Coum-H^\bullet and $\text{NPG}_{(-\text{H})}^\bullet$). $\text{NPG}_{(-\text{H},-\text{CO}_2)}^\bullet$ is produced by decarboxylation of $\text{NPG}_{(-\text{H})}^\bullet$; this decarboxylated compound can lead to the generation of reactive species (Ar^\bullet and $\text{NPG}_{(-\text{H},-\text{CO}_2)}^{\bullet+}$) by interaction with Iod salt (r6–r7). Therefore, the reactions r1–r7 are proposed for the three-component systems, and Ar^\bullet and $\text{NPG}_{(-\text{H},-\text{CO}_2)}^\bullet$ are the main species responsible for FRP.





3.2.4. Structure/Reactivity/Efficiency Relationship

During the FRP process, Coum1 and Coum2 proved to be efficient photoinitiators, as demonstrated by the remarkable polymerization profiles evidencing the high rates of reaction and the high final conversions of the acrylate functions. However, this was not the case for Coum3, which showed a lower efficiency during the FRP experiments despite the high molar extinction coefficient and the high electron transfer quantum yields of this coumarin. These counter-intuitive results can be related to the poor solubility of Coum3 in the monomers, as the addition a few drops of chloroform was required to increase the final conversion rate and the polymerization rate, resulting from the higher solubility of Coum3. Therefore, in light of the polymerization efficiency, Coum3 seems to have a low reactivity compared to Coum1 and Coum2. From the chemical structure point of view, Coum3 is a combination of Coum1 and Coum2, and the steric hindrance in Coum3 can clearly explain the poor reactivity of coum3. Thus, when using Coum3 in bulk, the diffusion is less favorable for all reactions in the multicomponent systems.

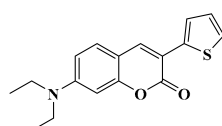
The better reactivity of Coum2 compared to Coum1 using two- or three-component photoinitiating systems for the photopolymerization of acrylate functions in thin samples can be explained by their differences in absorption properties. In fact, Coum2 exhibited a higher molar extinction coefficient at 405 nm compared with Coum1 ($\text{M}^{-1} \text{cm}^{-1}$ vs. $23,000 \text{M}^{-1} \text{cm}^{-1}$).

4. Experimental Part

4.1. Synthesis of Coumarins

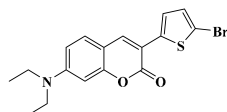
Details concerning analyses of the different compounds (NMR machines, mass spectroscopy, etc ...) described below have been reported in previous work [26].

4.1.1. Synthesis of 7-(Diethylamino)-3-(thiophen-2-yl)-2H-chromen-2-one 3

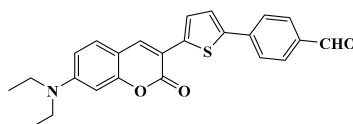


Thiopheneacetic acid **2**. (7.80 g, 55 mmol, $M = 142.17 \text{ g/mol}$), 4-(diethylamino)salicylaldehyde **1** (16.4 g, 85 mmol, $M = 193.24 \text{ g/mol}$) were dissolved in acetic anhydride (200 mL). Triethylamine (14.6 mL, 105 mmol) was added, and the solution was refluxed for three hours. After cooling, water was added. The aqueous phase was extracted several times with AcOEt. The organic layers were combined, dried over magnesium sulfate, and the solvent was removed under reduced pressure. The residue was purified by flash column chromatography (SiO_2 , DCM: pentane 1:1) to yield coumarin **3** as a yellow solid (14.0 g, 85% yield). ${}^1\text{H}$ NMR (CDCl_3) δ : 1.18 (t, 6H, $J = 7.1 \text{ Hz}$), 3.39 (q, 4H, $J = 7.1 \text{ Hz}$), 6.50 (d, 1H, $J = 2.4 \text{ Hz}$), 6.57 (dd, 1H, $J = 8.8 \text{ Hz}$, $J = 2.4 \text{ Hz}$), 7.04 (t, 1H, $J = 3.8 \text{ Hz}$), 7.26–7.29 (m, 2H), 7.62 (d, 1H, $J = 3.7 \text{ Hz}$), 7.83 (s, 1H); ${}^{13}\text{C}$ NMR (CDCl_3) δ : 12.5, 44.9, 97.2, 108.8, 109.3, 114.9, 124.9, 125.5, 127.2, 128.8, 136.8, 137.5, 150.5, 155.6, 160.5; HRMS (ESI MS) m/z : theor: 299.0980 found: 299.0982 (M^+ . detected). Analyses were consistent with those reported in the literature [27–29].

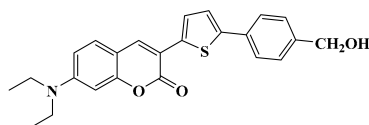
4.1.2. Synthesis of 3-(5-Bromothiophen-2-yl)-7-(Diethylamino)-2H-chromen-2-one 4



N-bromosuccinimide (NBS) (2.6 g, 14.69 mmol, $M = 177.98 \text{ g/mol}$) was added to a solution of 7-(diethylamino)-3-(thiophen-2-yl)-2*H*-chromen-2-one 3 (4.0 g, 13.36 mmol, $M = 299.39 \text{ g/mol}$) in THF (120 mL). The mixture was stirred at room temperature for 4 h, and water (20 mL) was added. The mixture was extracted with CH_2Cl_2 several times. The combined organic phases were combined, dried over magnesium sulfate, and the solvent removed under reduced pressure. The residue was purified by precipitation in a mixture diethyl ether/pentane. It was isolated as a yellow solid (3.74 g, 74% yield). $^1\text{H NMR}$ (CDCl_3) δ : 1.21 (t, 6H, $J = 7.1 \text{ Hz}$), 3.43 (q, 4H, $J = 7.1 \text{ Hz}$), 6.52 (d, 1H, $J = 1.9 \text{ Hz}$), 6.62 (dd, 1H, $J = 8.8 \text{ Hz}$, $J = 1.9 \text{ Hz}$), 7.03 (d, 1H, $J = 4.0 \text{ Hz}$), 7.30–7.33 (m, 2H), 7.82 (s, 1H); $^{13}\text{C NMR}$ (CDCl_3) δ : 12.5, 44.9, 97.2, 108.6, 109.5, 113.2, 114.1, 124.0, 129.7, 136.1, 138.7, 150.7, 155.5, 160.5; HRMS (ESI MS) m/z : theor: 377.0085 found: 377.0088 (M^+ . detected). Analyses were consistent with those reported in the literature [30,31].

4.1.3. Synthesis of 4-(5-(7-(Diethylamino)-2-oxo-2*H*-chromen-3-yl)thiophen-2-yl)benzaldehyde 5

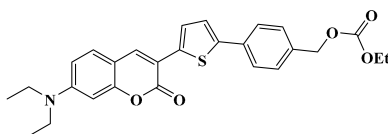
Tetrakis(triphenylphosphine)palladium (0) (0.46 g, 0.744 mmol, $M = 1155.56 \text{ g.mol}^{-1}$) was added to a mixture of 3-(5-bromothiophen-2-yl)-7-(diethylamino)-2*H*-chromen-2-one 4 (2.31 g, 6.11 mmol, $M = 378.28 \text{ g mol}^{-1}$), (4-formylphenyl)boronic acid (1.37 g, 9.16 mmol, $M = 149.94 \text{ g mol}^{-1}$), toluene (54 mL), ethanol (26 mL), and an aqueous K_2CO_3 solution (2 M, 6.91 g in 25 mL water, 26 mL) under vigorous stirring. The mixture was stirred at 80°C for 48 h under a nitrogen atmosphere. After cooling to room temperature, the reaction mixture was poured into water and extracted with ethyl acetate. The organic layer was washed with brine several times, and the solvent removed under reduced pressure. The residue was purified by filtration on a plug of silica gel using a mixture of DCM/ethanol as the eluent. The product was isolated with 88% yield (1.23 g). $^1\text{H NMR}$ (CDCl_3) δ : 1.24 (t, 6H, $J = \text{Hz}$), 3.44 (q, 4H, $J = \text{Hz}$), 6.54 (d, 1H, $J = 2.2 \text{ Hz}$), 6.63 (dd, 1H, $J = 8.8 \text{ Hz}$, $J = 2.4 \text{ Hz}$), 7.34 (d, 1H, $J = 8.8 \text{ Hz}$), 7.45 (d, 1H, $J = 4.0 \text{ Hz}$), 7.65 (d, 1H, $J = 4.0 \text{ Hz}$), 7.80 (d, 1H, $J = 8.3 \text{ Hz}$), 7.88 (d, 1H, $J = 8.3 \text{ Hz}$), 7.94 (s, 1H), 9.99 (s, 1H, CHO); $^{13}\text{C NMR}$ (CDCl_3) δ : 12.5, 44.9, 97.2, 108.7, 109.5, 114.1, 125.3, 125.7, 129.1, 130.4, 134.9, 136.8, 139.2, 140.2, 142.2, 150.8, 155.7, 160.4, 191.4; HRMS (ESI MS) m/z : theor: 403.1242 found: 403.1245 (M^+ . detected).

4.1.4. Synthesis of 7-(Diethylamino)-3-(5-(4-(hydroxymethyl)phenyl)thiophen-2-yl)-2*H*-chromen-2-one Coum1

4-(5-(7-(Diethylamino)-2-oxo-2*H*-chromen-3-yl)thiophen-2-yl)benzaldehyde 5 (0.5 g, 1.24 mmol, 403.49 g/mol) was suspended in a mixture of ethanol/THF (100/200 mL), and sodium borohydride (100 mg) was added. The solution was stirred at room temperature for 1.5 h (TLC control). The solution

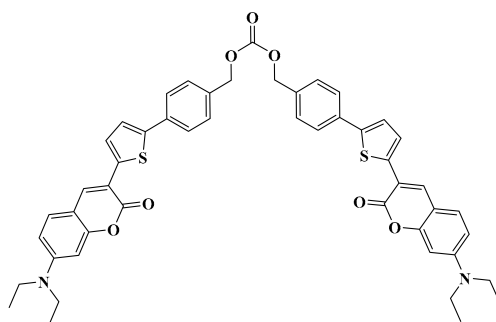
was quenched with HCl (1 mL, 1M), and the solvent was removed under reduced pressure. The residue was filtered on a plug of silica gel using THF as the eluent. The product (Coum1) was isolated in quantitative yield. ^1H NMR (CDCl_3) δ : 1.22 (t, 6H, $J = 7.1$ Hz), 3.44 (q, 4H, $J = 7.1$ Hz), 4.72 (d, 2H, $J = 3.7$ Hz), 5.00 (s, 1H), 6.54 (d, 1H, $J = 2.4$ Hz), 6.62 (dd, 1H, $J = 8.8$ Hz, $J = 2.4$ Hz), 7.30–7.40 (m, 4H), 7.63–7.67 (m, 3H), 7.90 (s, 1H); ^{13}C NMR (CDCl_3) δ : 12.5, 21.2, 30.3, 34.2, 44.9, 65.1, 97.2, 108.8, 109.3, 114.7, 123.4, 125.5, 125.81, 125.83, 127.5, 128.3, 128.8, 132.6, 133.9, 135.8, 136.3, 136.9, 140.1, 143.7, 150.5, 151.5, 155.6, 160.5; HRMS (ESI MS) m/z : theor: 405.1399 found: 405.1396 (M^+ . detected).

4.1.5. Synthesis of 4-(5-(7-(Diethylamino)-2-oxo-2H-chromen-3-yl) thiophen-2-yl) benzyl ethyl carbonate Coum2



To a solution of 7-(diethylamino)-3-(5-(4-(hydroxymethyl)phenyl)thiophen-2-yl)-2H-chromen-2-one Coum1 (405 mg, 10 mmol, $M = 405.51$ g/mol) and pyridine (0.87 g, 0.89 mL, 11 mmol, $M = 79.10$ g/mol, $d = 0.978$) in dichloromethane (DCM) (60 mL), 0 °C ethyl chloroformate (1.95 g, 1.72 mL, 18 mmol, $M = 108.52$ g/mol, $d = 1.135$) was added dropwise. The solution was stirred at room temperature for two hours. 1 M HCl (30 mL) was added to the solution, and the aqueous phase was extracted several times with dichloromethane. The organic phases were combined, dried over magnesium sulfate, and the solvent removed under reduced pressure. The residue was purified by column chromatography (SiO_2) using a gradient of eluent from pentane to DCM (415 mg, 87% yield). ^1H NMR (CDCl_3) δ : 1.22 (t, 6H, $J = 7.1$ Hz), 1.32 (t, 3H, $J = 7.1$ Hz), 3.42 (q, 4H, $J = 7.1$ Hz), 4.22 (q, 2H, $J = 7.1$ Hz), 6.52 (d, 1H, $J = 2.4$ Hz), 6.60 (dd, 1H, $J = 8.8$ Hz, $J = 2.4$ Hz), 7.27–7.30 (m, 2H), 7.39 (d, 2H, $J = 8.2$ Hz), 7.61–7.66 (m, 3H), 7.88 (s, 1H); ^{13}C NMR (CDCl_3) δ : 12.5, 14.3, 44.9, 64.2, 69.1, 97.1, 108.8, 109.3, 114.5, 123.7, 125.70, 125.72, 128.91, 128.93, 134.4, 134.6, 136.4, 137.2, 143.4, 150.6, 155.1, 155.5, 160.4; HRMS (ESI MS) m/z : theor: 477.1610 found: 477.1613 (M^+ . detected)

4.1.6. Synthesis of bis (4-(5-(7-(Diethylamino)-2-oxo-2H-chromen-3-yl) thiophen-2-yl)benzyl) carbonate Coum3



To a solution of 7-(Diethylamino)-3-(5-(4-(hydroxymethyl)phenyl)-thiophen-2-yl)-2H-chromen-2-one Coum2 (5.25 g, 12.95 mmol, 2.1 eq., $M = 405.51$ g/mol) in dry THF (50 mL) was added in small portions at 0 °C sodium hydride 95% (0.32 g, 12.64 mmol, 2.05 eq., $M = 24$ g/mol). The solution was allowed to warm to room temperature and stirring was maintained for 2 h. Then, 1,1'-carbonyldiimidazole (CDI) (1 g, 6.17 mmol, 1 eq., $M = 162.15$ g/mol) was slowly added at 0 °C, and the reaction was refluxed overnight. After cooling, the reaction was quenched by the addition of water, and THF was removed under reduced pressure. The aqueous phase was extracted with DCM several times. The organic phases were combined, dried over magnesium sulfate, and the solvent

removed under reduced pressure. The residue was purified by column chromatography (SiO₂) using a gradient of eluent from pentane to DCM (4.03 g, 78% yield). ¹H NMR (CDCl₃) δ: 1.21 (t, 12H, J = 7.1 Hz), 3.43 (q, 8H, J = 7.1 Hz), 5.19 (s, 4H), 6.53 (d, 2H, J = 2.4 Hz), 6.62 (dd, 2H, J = 8.8 Hz, J = 2.4 Hz), 7.30–7.34 (m, 4H), 7.39 (d, 4H, J = 8.4 Hz), 7.63–7.67 (m, 6H), 7.89 (s, 2H); ¹³C NMR (CDCl₃) δ: 12.5, 44.9, 69.5, 97.2, 108.8, 109.3, 114.6, 123.7, 125.7, 125.8, 128.9, 129.0, 134.2, 134.7, 136.4, 137.2, 143.4, 150.6, 155.1, 155.6, 160.4; HRMS (ESI MS) m/z: theor: 836.2590 found: 836.2595 (M⁺. detected)

4.2. Other Chemicals

The different additives used in this work were purchased from Lambson Ltd. (Wetherby, UK), Sigma Aldrich (St. Quentin Fallavier, France) or TCI Europe (Paris, France). The two monomers were obtained from Allnex. Chemical structures of monomers and additives are shown in Scheme 2.

4.3. Light Sources

The following light sources were used in this work: (1) LED @ 375 nm (I = 40 mW cm⁻²) (2) LED @ 405 nm (I = 110 mW.cm⁻²).

4.4. Free Radical Photopolymerization (FRP)

Coumarin/Iod (0.05–0.1%/1% w/w) or coumarin/Iod/additive (0.05–0.1%/1%/1 w/w/w) combinations were used as photoinitiating systems for the FRP of acrylates. Percentages mentioned for the different chemical compounds and used in the photoinitiating systems are related to the monomer weight.

FRP of TMPTA and TA was performed under laminated conditions (~25 μm thickness) to reduce O₂ inhibition. For thick samples (1.4 mm of thickness), the formulations were polymerized in a plastic mold ~1 cm in diameter. Monomer conversions (TMPTA or TA) were continuously followed by real-time FTIR spectroscopy. More details about photopolymerization monitoring are provided in [32,33].

4.5. Redox Potentials

Experimental conditions and equipment were previously detailed in Reference [34].

4.6. Fluorescence Experiments

Experimental conditions and equipment were previously detailed in Reference [34].

4.7. UV-Visible Absorption and Photolysis Experiments

Experimental conditions and equipment were previously detailed in Reference [34].

4.8. Computational Procedure

Theoretical calculations were carried out under the conditions previously detailed [35,36].

4.9. 3D Printing Experiments

A diode laser at 405 nm was used for 3D printing experiments, with light intensity similar to that used in the IR experiments. Polymerization was carried out under air. Analyses were performed with a numerical optical microscope (Shinjuku, Japan) (DSX-HRSU from OLYMPUS Corporation) [37].

4.10. Near-UV Conveyor

Photocomposite synthesis was carried out by impregnating the TMPTA- or the TA-based resin with glass fibers (resin/fibers: 50%/50% w/w). Then, the glass fiber/resin system was irradiated using a dymax-LED conveyor. Other experimental conditions (belt speed, distance between the light source and the sample) were previously detailed in reference [34].

5. Conclusions

In this paper, a series of coumarins have been proposed as efficient photoinitiators for the free radical polymerization of acrylates at 405 nm. Interestingly, the third coumarin (Coum3) examined as a photoinitiator proved to be a poor candidate, mainly attributable to its lack of solubility in the photocurable resins and its bulky character. Here again, the crucial role of molecular engineering for the design of highly efficient photoinitiators has been clearly evidenced. The best coumarins were tested for 3D printing experiments at 405 nm and for the synthesis of photocomposites with significant hardening of the surface and on the bottom using an LED @ 385 nm. In light of the high efficiency of coumarins, future development will consist of designing coumarins absorbing in the near infrared range, where light penetration is more important than that in the near UV/visible range.

Author Contributions: Conceptualization, J.L., F.D., M.R.; methodology, J.L., H.M., M.R.; J.T., T.H.; synthesis of dyes, F.D.; software, B.G.; validation, all authors; formal analysis, J.L., M.R., H.M., F.D.; data curation, all authors; writing—original draft preparation, J.L., M.R., H.M., F.D., J.T., T.H.; writing—review and editing, all authors. All authors have read and agreed to the published version of the manuscript.

Funding: Association of Specialization and Scientific Guidance.

Acknowledgments: The Lebanese group would like to thank “The Association of Specialization and Scientific Guidance” (Beirut, Lebanon) for funding and supporting this scientific work. This work was granted access to the HPC resources of the Mesocentre of the University of Strasbourg.

Conflicts of Interest: The authors declare no conflict of interest.

References

1. Ueno, K.; Oshikiri, T.; Sun, Q.; Shi, X.; Misawa, H. Solid-State Plasmonic Solar Cells. *Chem. Rev.* **2018**, *118*, 2955–2993. [[CrossRef](#)]
2. Fouassier, J.-P.; Morlet-Savary, F.; Lalevée, J.; Allonas, X.; Ley, C. Dyes as photoinitiators or photosensitizers of polymerization reactions. *Materials* **2010**, *3*, 5130–5142. [[CrossRef](#)]
3. Fouassier, J.-P.; Lalevée, J. *Photoinitiators for Polymer Synthesis, Scope, Reactivity, and Efficiency*; Wiley-VCH Verlag GmbH & Co.KGaA: Weinheim, Germany, 2012.
4. Fouassier, J.-P. *Photoinitiator, Photopolymerization and Photocuring: Fundamentals and Applications*; Hanser Gardner: New York, NY, USA, 1995.
5. Xiao, P.; Zhang, J.; Dumur, F.; Tehfe, M.-A.; Morlet-Savary, F.; Graff, B.; Gigmes, D.; Fouassier, J.-P.; Lalevée, J. Photoinitiating systems: Recent progress in visible light induced cationic and radical photopolymerization reactions under soft conditions. *Prog. Polym. Sci.* **2015**, *41*, 32–66. [[CrossRef](#)]
6. Trykowska-Konc, J.; Hejchman, E.; Kruszevska, H.; Wolska, I.; Maciejewska, D. Synthesis and pharmacological activity of O-aminoalkyl derivatives of 7-hydroxycoumarin. *Eur. J. Med. Chem.* **2011**, *46*, 2252–2263. [[CrossRef](#)]
7. Wattenberg, L.W.; Low, L.K.T.; Fladmoe, A.V. Inhibition of chemical carcinogen-induced neoplasia by coumarins and α -angelicalactone. *Cancer Res.* **1979**, *39*, 1651–1654.
8. Manolov, I.; Kostova, I.; Netzeva, T.; Konstantinov, S.; Karaivanova, M. Cytotoxic activity of cerium complexes with coumarin derivatives. Molecular modeling of the ligands. *Archiv. Pharm. Med. Chem.* **2000**, *333*, 93–98. [[CrossRef](#)]
9. Lake, B.G. Coumarin metabolism, toxicity and carcinogenicity: Relevance for human risk assessment. *Food Chem. Toxicol.* **1999**, *37*, 423–453. [[CrossRef](#)]
10. Manojkumar, P.; Ravi, T.K.; Subbuchettiar, G. Synthesis of coumarin heterocyclic derivatives with antioxidant activity and in vitro cytotoxic activity against tumour cells. *Acta Pharm.* **2009**, *59*, 159–170. [[CrossRef](#)] [[PubMed](#)]
11. Mayekar, S.A.; Chaskar, A.C.; Mulwad, V.V. Facile synthesis of coumarinyl isothiocyanate from amino coumarin. *Synth. Commun.* **2009**, *40*, 46–51. [[CrossRef](#)]
12. Jiang, Z.-J.; Lv, H.-S.; Zhu, J.; Zha, B.-X. New fluorescent chemosensor based on quinoline and coumarin for Cu^{2+} . *Synth. Met.* **2012**, *162*, 2112–2116. [[CrossRef](#)]
13. Aldakov, D.; Anzenbacher, P. Dipyrrolyl quinoxalines with extended chromophores are efficient fluorimetric sensors for pyrophosphate. *Chem. Commun.* **2003**, *12*, 1394–1395. [[CrossRef](#)]

14. Hunger, K. *Industrial Dyes*, WILEY-VCH Verlag; Gmbh & Co. KGaA: Weinheim, Germany, 2003.
15. Su, K.; Ming, J.; Zhang, L.; Xiang, S.; Cui, M.; Yang, H. A novel tricyclic heterocyclic fluorescent probe for Pd²⁺ in aqueous solution: Synthesis, properties and theoretical calculations. *Opt. Mater.* **2019**, *93*, 25–29. [[CrossRef](#)]
16. Nasser Mabkhot, Y.; Barakat, A.; Mohammed Al-Majid, A.; Alshahrani, S.; Yousuf, S.; Iqbal Choudhary, M. Synthesis, reactions and biological activity of some new bis-heterocyclic ring compounds containing sulphur atom. *Chem. Cent. J.* **2013**, *7*, 112. [[CrossRef](#)] [[PubMed](#)]
17. Cabanetos, C.; Blanchard, P.; Roncali, J. Arylamine Based Photoactive Push-Pull Molecular Systems: A Brief Overview of the Chemistry “Made in Angers”. *Chem. Rec.* **2019**, *19*, 1123–1130. [[CrossRef](#)]
18. Tehfe, M.-A.; Dumur, F.; Graff, B.; Morlet-Savary, F.; Gignes, D.; Fouassier, J.-P.; Lalevée, J. Push-pull (thio)barbituric acid derivatives in dye photosensitized radical and cationic polymerization reactions under 457/473 nm Laser beams or blue LEDs. *Polym. Chem.* **2013**, *4*, 3866–3875. [[CrossRef](#)]
19. Xiao, P.; Dumur, F.; Graff, B.; Vidal, L.; Gignes, D.; Fouassier, J.-P.; Lalevée, J. Structural effects in the indanedione skeleton for the design of low intensity 300–500 nm light sensitive initiators. *Macromolecules* **2014**, *47*, 26–34. [[CrossRef](#)]
20. Xiao, P.; Dumur, F.; Tehfe, M.-A.; Gignes, D.; Fouassier, J.-P.; Lalevée, J. Red-light-induced cationic photopolymerization: Perylene derivatives as efficient photoinitiators. *Macromol. Rapid Commun.* **2013**, *34*, 1452–1458. [[CrossRef](#)]
21. Dumur, F.; Gignes, D.; Fouassier, J.-P.; Lalevée, J. Organic Electronics: An El Dorado in the quest of new photocatalysts as photoinitiators of polymerization. *Acc. Chem. Res.* **2016**, *49*, 1980–1989. [[CrossRef](#)]
22. Xiao, P.; Hong, W.; Li, Y.; Dumur, F.; Graff, B.; Fouassier, J.-P.; Gignes, D.; Lalevée, J. Green light sensitive diketopyrrolopyrrole derivatives used in versatile photoinitiating systems for photopolymerizations. *Polym. Chem.* **2014**, *5*, 2293–2300. [[CrossRef](#)]
23. Dietlin, C.; Schweizer, S.; Xiao, P.; Zhang, J.; Morlet-Savary, F.; Graff, B.; Fouassier, J.-P.; Lalevée, J. Photopolymerization upon LEDs: New photoinitiating systems and strategies. *Polym. Chem.* **2015**, *6*, 3895–3912. [[CrossRef](#)]
24. Zhang, J.; Zivic, N.; Dumur, F.; Guo, C.; Li, Y.; Xiao, P.; Graff, B.; Gignes, D.; Fouassier, J.-P.; Lalevée, J. Panchromatic photoinitiators for radical, cationic and thiol-ene polymerization reactions: A search in the diketopyrrolopyrrole or indigo dye series. *Mater. Today Commun.* **2015**, *4*, 101–108. [[CrossRef](#)]
25. Al Mousawi, A.; Poriel, C.; Dumur, F.; Toufaily, J.; Hamieh, T.; Fouassier, J.-P.; Lalevée, J. Zinc tetraphenylporphyrin as high performance visible-light photoinitiator of cationic photosensitive resins for LED projector 3D printing applications. *Macromolecules* **2017**, *50*, 746–753. [[CrossRef](#)]
26. Telitel, S.; Dumur, F.; Campolo, D.; Poly, J.; Gignes, D.; Fouassier, J.-P.; Lalevée, J. Iron complexes as potential photocatalysts for controlled radical photopolymerizations: A tool for modifications and patterning of surfaces. *J. Polym. Sci. A Polym. Chem.* **2016**, *54*, 702–713. [[CrossRef](#)]
27. Gualandi, A.; Rodeghiero, G.; Della Rocca, E.; Bertoni, F.; Marchini, M.; Perciaccante, R.; Jansen, T.P.; Ceroni, P.; Cozzi, P.G. Application of coumarin dyes for organic photoredox catalysis. *Chem. Commun.* **2018**, *54*, 10044–10047. [[CrossRef](#)]
28. Liu, L.; Huang, D.; Draper, S.M.; Yi, X.; Wu, W.; Zhao, J. Visible light-harvesting trans bis(alkylphosphine)platinum(II)-alkynyl complexes showing long-lived triplet excited states as triplet photosensitizers for triplet-triplet annihilation upconversion. *Dalton Trans.* **2013**, *42*, 10694–10706. [[CrossRef](#)]
29. Kotchapadist, P.; Prachumrak, N.; Sunonnam, T.; Namuangruk, S.; Sudyoadsuk, T.; Keawin, T.; Jungsuttiwong, S.; Promarak, V. Synthesis, characterisation, and electroluminescence properties of n-coumarin derivatives containing peripheral triphenylamine. *Eur. J. Org. Chem.* **2015**, *3*, 496–505. [[CrossRef](#)]
30. Yu, T.; Zhu, Z.; Bao, Y.; Zhao, Y.; Liu, X.; Zhang, H. Investigation of novel carbazole-functionalized coumarin derivatives as organic luminescent materials. *Dyes Pigm.* **2017**, *147*, 260–269. [[CrossRef](#)]
31. Kochapradist, P.; Sunonnam, T.; Prachumrak, N.; Namuangruk, S.; Keawin, T.; Jungsuttiwong, S.; Sudyoadsuk, T.; Promarak, V. Synthesis, characterization, and properties of novel bis(aryl)carbazole-containing N-coumarin derivatives. *Tetrahedron Lett.* **2014**, *55*, 6689–6693. [[CrossRef](#)]
32. Al Mousawi, A.; Kermagoret, A.; Versace, D.-L.; Toufaily, J.; Hamieh, T.; Graff, B.; Dumur, F.; Gignes, D.; Fouassier, J.-P.; Lalevée, J. Copper photoredox catalysts for polymerization upon near UV or visible light: Structure/reactivity/efficiency relationships and use in LED projector 3D printing resins. *Polym. Chem.* **2016**, *8*, 568–580. [[CrossRef](#)]

33. Al Mousawi, A.; Dietlin, C.; Graff, B.; Morlet-Savary, F.; Toufaily, J.; Fouassier, J.-P.; Chachaj-Brekiesz, A.; Ortyl, J.; Lalevée, J. Meta-terphenyl derivative/iodonium salt/9H-carbazole-9-ethanol photoinitiating systems for free radical promoted cationic polymerization upon visible lights. *Macromol. Chem. Phys.* **2016**, *217*, 1955–1965. [[CrossRef](#)]
34. Abdallah, M.; Hijazi, A.; Graff, B.; Fouassier, J.-P.; Rodeghiero, G.; Gualandi, A.; Dumur, F.; Cozzi, P.G.; Lalevée, J. Coumarin derivatives as versatile photoinitiators for 3D printing, polymerization in water and photocomposite synthesis. *Polym. Chem.* **2019**, *10*, 872–884. [[CrossRef](#)]
35. Bonardi, A.-H.; Bonardi, F.; Noirbent, G.; Dumur, F.; Dietlin, C.; Gigmes, D.; Fouassier, J.-P.; Lalevée, J. Different NIR dye scaffolds for polymerization reactions under NIR light. *Polym. Chem.* **2019**, *10*, 6505–6514. [[CrossRef](#)]
36. Tehfe, M.-A.; Dumur, F.; Xiao, P.; Delgove, M.; Graff, B.; Gigmes, D.; Fouassier, J.-P.; Lalevée, J. Chalcone derivatives as highly versatile photoinitiators for radical, cationic, thiol-ene and IPN polymerization reactions upon visible lights. *Polym. Chem.* **2014**, *5*, 382–390. [[CrossRef](#)]
37. Zhang, J.; Dumur, F.; Xiao, P.; Graff, B.; Bardelang, D.; Gigmes, D.; Fouassier, J.-P.; Lalevée, J. Structure design of naphthalimide derivatives: Toward versatile photoinitiators for near-UV/visible LEDs, 3D printing, and water-soluble photoinitiating systems. *Macromolecules* **2015**, *48*, 2054–2063. [[CrossRef](#)]

Publisher's Note: MDPI stays neutral with regard to jurisdictional claims in published maps and institutional affiliations.



© 2020 by the authors. Licensee MDPI, Basel, Switzerland. This article is an open access article distributed under the terms and conditions of the Creative Commons Attribution (CC BY) license (<http://creativecommons.org/licenses/by/4.0/>).